SCIENTIFIC REPORTS

OPEN

SUBJECT AREAS:
SOLAR CELLS
CIVIL ENGINEERING

Received
15 July 2013

Accepted
16 August 2013

Published
25 September 2013

Correspondence and requests for materials should be addressed to N.K. (nkouklin@uwm.edu)

Concrete Embedded Dye-Synthesized Photovoltaic Solar Cell

T. Hosseini[1], I. Flores-Vivian[2], K. Sobolev[2,3] & N. Kouklin[1]

[1]Department of Electrical Engineering, [2]Department of Civil Engineering & Mechanics, [3]Department of Materials Science, University of Wisconsin-Milwaukee, Milwaukee, WI 53211, USA.

This work presents the concept of a monolithic concrete-integrated dye-synthesized photovoltaic solar cell for optical-to-electrical energy conversion and on-site power generation. The transport measurements carried out in the dark revealed the presence of V_{OC} of ~190 mV and I_{SC} of ~9 μA, induced by the electrochemical conversion of concrete-supplied ionic impurities at the electrodes. The current-voltage measurements performed under illumination at incident optical powers of ~46 mW confirmed the generation of electrical power of ~0.64 μW with almost half generated via battery effect. This work presents a first step towards realizing the additional pathways to low-cost electrical power production in urban environments based on a combined use of organic dyes, nanotitania and concrete technology.

Concrete represents one of the oldest material technologies that has the widespread use in civil and infrastructure applications due to its high compressive strength and exceptional durability achieved at a relatively low production costs[1–4]. On the other side, the "land take," the expansion of residential areas and construction sites, is the predominant reason for the increase in concrete coverage of urban land and loss of natural ecosystems[5,6]. In the United States alone, the concrete expansion rate exceeds ca. 250,000 million acres per year. With continued intensification of urbanization, a considerable CO_2 footprint of commercial and residential buildings is associated with ever-increasing levels of energy consumption by the building occupants, thereby requiring innovative architectural and engineering approaches to the direct production of electrical energy under urban constraints[5]. To this end, realizing the solar energy harvesting capabilities of concrete surfaces can offer multiple benefits, including onsite power generation to offset power delivery losses and fewer cooling requirements while obviating the need for developing additional power generating and grid infrastructure[6].

In addition, modern architectural design frequently incorporates decorative concrete surfaces, which are ideal for deploying concrete-embedded photovoltaic systems. These systems, when supplemented with batteries for energy storage, can supply electrical power uninterruptedly, i.e., 24-hours per day. When it comes to household energy consumption metrics, the solar energy harvesting technologies with a marginally acceptable efficiency-to-cost ratio can be considered economically acceptable as long as they can generate enough on-site electrical power and remain scalable[5]. Here, for the first time, we propose and explore the concept of monolithic concrete-incorporated dye-synthesized solar cells. The prototype cells were developed as a top surface layer of a thin concrete tile. As a part of the proof-of-the concept experiments, the current-voltage (I–V) characteristics of the cell prototypes were obtained by carrying out photo-current-voltage tests, and the results were used to extract the efficiency and fill factor characteristics, as further described in this paper.

Most of the recent research in cement and concrete technology has concentrated on improving the mechanical characteristics of the resultant concrete structures; however, more recently, additional pathways to developing concrete with novel value-added functionalities were suggested[1,2,7,8]. Examples include incorporating TiO_2 nanoparticles in photo-catalytic concrete that is capable of air depollution (e.g., by reducing NO_x upon exposure to UV-light) and self-cleaning[1,2]. The work described here presents a step forward in developing multi-functional, zero CO_2 footprint concrete product derivatives with novel solar-to-electrical power conversion capabilities.

The concept of low-cost, photovoltaic dye-synthesized solar cells (DSSC) with relatively high efficiencies of 10+% that can be printed/painted on large areas continues to gain interest[8,9]. The light absorption and, in turn, external cell conversion efficiency, is dependent on the molar extinction coefficient of the dye, surface coverage by the dye, and net effective surface area/depth. Importantly, only DSSCs that feature a mesoporous TiO_2 electrode design are known to demonstrate a larger operational efficiency by a factor of ~1000 compared with planar counterparts. The TiO_2 nanoparticles can be successfully integrated into a porous cementitious matrix[1,2,7,10,11], making the TiO_2 based DSSC the best candidate for realizing solar energy harvesting concrete.

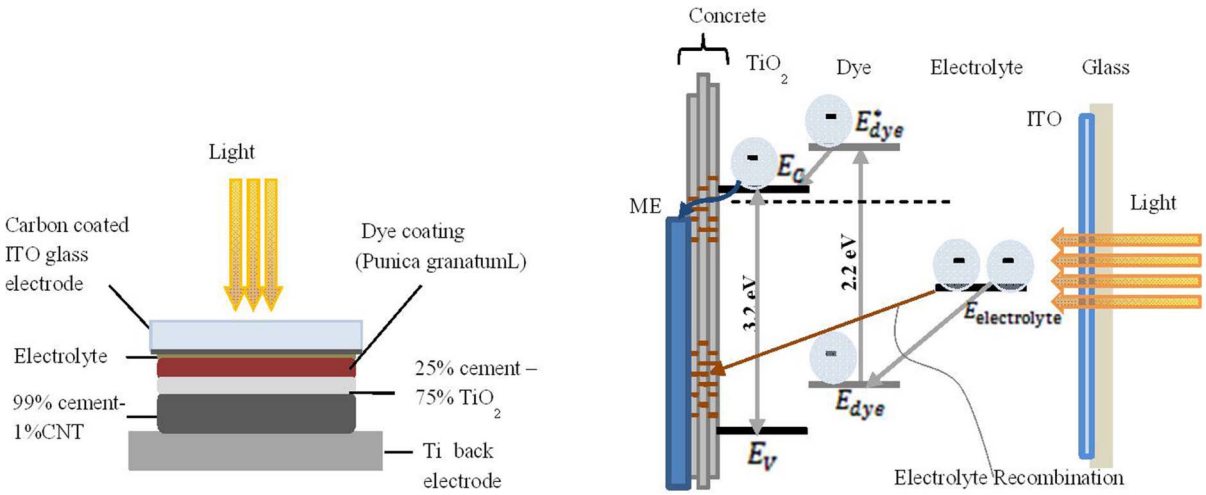

Figure 1 | (Left) The schematics of the concrete-dye solar cell and (right) the energy band diagram describing the PV-effect and electrical power generation in concrete-dye solar cells. The device part of concrete is represented by a set of interconnected crystallites featuring surface defect states that serve as transport channels for photo-carriers likely involving hopping and thermally-assisted tunneling.

Results

The multi-layer structure of the electrolyte-based concrete-dye cell is schematically presented in Figure 1(a). The Ti maps obtained on the cross-section of the concrete, the structure of TiO_2-concrete via scanning electron microscopy (SEM), Figure 2(c), and energy dispersive spectroscopy (EDS), Figure 2(d) confirm the formation of an almost abrupt, well-defined materials junction between the conductive carbon nanotube (CNT) and TiO_2-based layers. This indicates that the effects of the diffusion of TiO_2 nanoparticles and layer mixing remain limited. According to Figure 2(c), both layers exhibit a highly compatible porous structure, a required condition for their seamless integration and added mechanical synergy.

Punica Granatum L (PGL) extract was deposited on the composite concrete tablet, resulting in a violet coloration of the concrete surface. The iodide/tri-iodide (I^-/I_3^-) solution was used as the electrolyte that filled the gap between the dye-sensitized concrete tablet and optically-transparent Indium Tin Oxide (ITO)-coated conducting glass (which serves as a counter electrode).

To confirm that PGL extract has proper light-harvesting characteristics, the photoluminescence (PL) spectroscopic tests were first performed on concentrated PGL extract derived from pomegranate seeds. Figure 3 shows the resultant PL spectrum which consists of three spectrally overlapping bands. The peaks at ~620, 660, and 720 nm are attributed to the zero-phonon PL line and its two vibronic progressions, respectively. Next, the photoluminescence excitation (PLE) measurements were accomplished by monitoring the PL emission at ~620 nm while performing spectral excitation scans in the spectral range of ~480–600 nm. The PL and PLE bands feature a narrow Stockes shift of ~50 nm, which can be beneficial in reducing emission-related losses via internal dye re-absorption in the spectral window of ~580–640 nm.

The position of the main PLE peak is generally consistent with that of natural dye compounds, e.g., anthocyanin, chlorophyll, and carotenoids[8]. The dye also is projected to have only weak absorption at the band-edge, i.e., around ca. 700 nm, which limits the spectral conversion to the near-infrared zone. According to the PLE data, Figure 3, the effective absorption bandwidth is limited to ~200 nm, with most of the absorption falling into visible spectral range starting from ~480 nm. Compared with Ruthenium (Ru)-based synthesizing complexes used in DSSC, the organic counterparts have a molar extinction coefficient on average of ca. 10^5 M^{-1} cm^{-1}, thus by a factor of 5–10 exceeding that of Ru-complexes[12,13]. The cell operation was tested by carrying out I–V measurements in the dark and by uniformly illuminating the cell with a *cw*-white light source with an emission spectrum of 420–650 nm and device adjusted incident optical power of ~46 mW. The I–V response was collected with a Keithley 236 source-measure unit; the results are plotted in Figure 4.

In the dark, the I–V characteristics are rectifying and show a presence of V_{OC} and I_{SC} approaching ca. 190 mV and 9 μA, respectively, indicating that the cell is initially not in an equilibrium state. An electrode work function difference remains a key driving force behind the electrical transport of concrete-supplied ionic impurities including K^+, Na^+ and Ca^{2+} towards ITO-electrode, where these can undergo an electrochemical conversion[14]. Since the concentration of CNTs is likely to be significantly below the percolated network threshold, the photo-generated charge carrier transport within the concrete matrix is likely to occur via hopping and thermally-assisted tunneling mechanisms that involve surface defect states in cementitious crystallites forming highly interconnected 3D-network, Figure 1 (right).

In the dark, the I–V characteristics are rectifying and show a presence of V_{OC} and I_{SC} approaching ca. 190 mV and 9 μA, respectively, indicating that even initially the cell is not in an equilibrium state. Electrical tests performed on Ti-electrolyte-ITO cells have not shown any measurable voltage, suggesting that the dark short circuit current and open circuit voltage are not associated with electrolyte electrochemical activity. On the other hand, according to previous cement hydration studies[2–4,14], a number of ions originating from KOH, NaOH and $Ca(OH)_2$ are released into interpore space when brought into the contact with the aqueous electrolyte.

At the ITO electrode (based on the example of K^+ ion):

$$K^+ + e \Rightarrow K^0$$

At the Ti-concrete electrode:

$$Ca + 2OH^- \Rightarrow Ca(OH)_2 + 2e$$

The formed alkali and hydroxide ions can diffuse out from the concrete surface against their concentration gradients and reach the counter (ITO) electrode. At steady-state, the positively charged alkali ions, similarly to triodine ions can undergo reduction at the ITO surface, whereas a neutral hydroxyl radical is formed by releasing an electron into an external circuit reacting with metal impurities at the ITO electrode. In the agreement with the experiment, the alkali ions experience continuous loss at the ITO surface; the surface becomes positively charged and biased positively in the absence of any illumination in reference to the Ti-concrete surface.

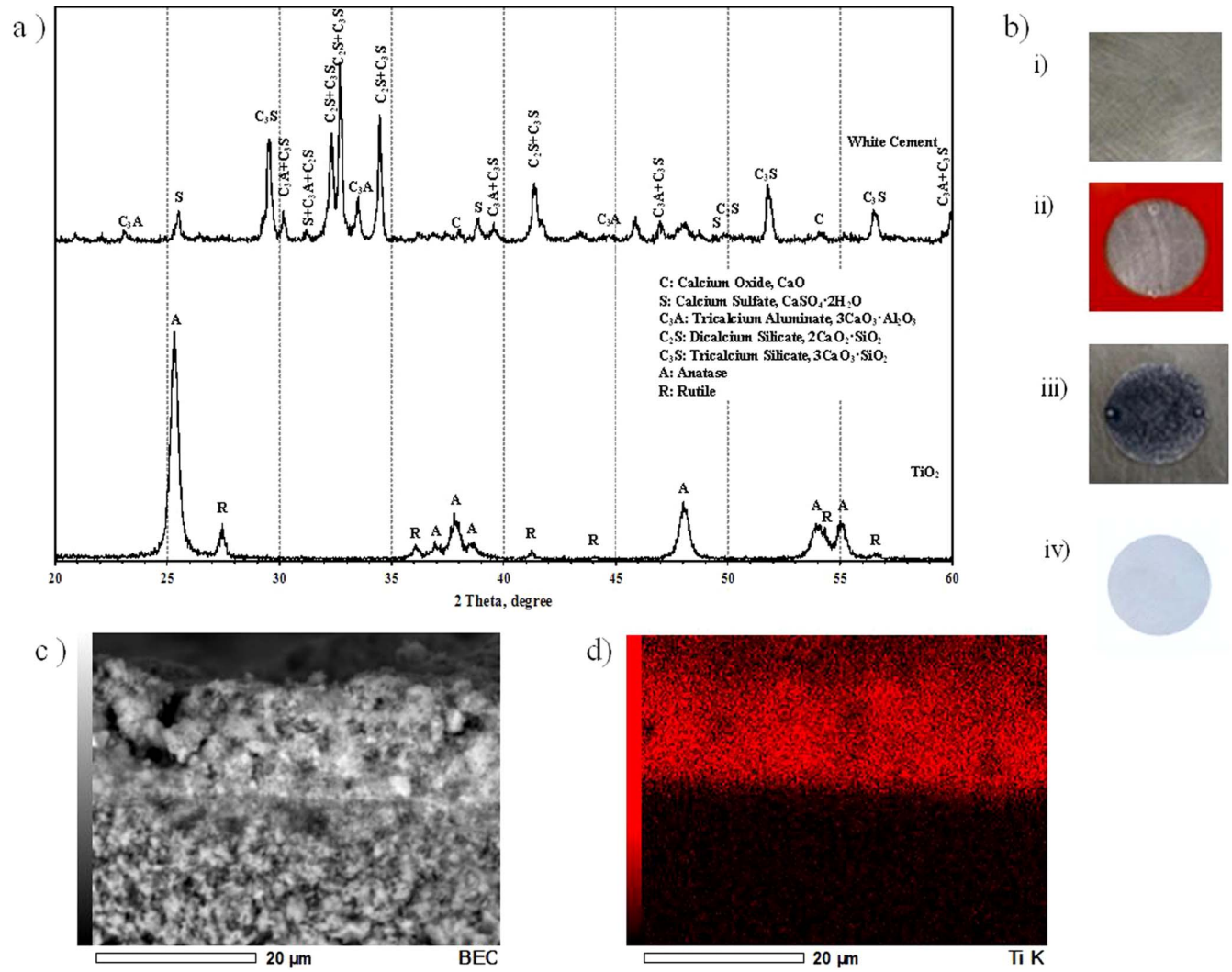

Figure 2 | (a) XRD spectra of white portland cement (top) and TiO_2 nanoparticles (bottom) used to engineer the cell; (b) Preparation of DSSC concrete specimen (i) titanium plate, (ii) the perfusion chamber mounted, (iii) hardened specimens, (iv) specimens coated with WPC-CNT layer; (c) Scanning electron microscopy; and (d) Energy-dispersive x-ray Ti map obtained on the interface of concrete and NT75 TiO_2-based layer.

Under illumination, both open-circuit voltage, V_{OC} and short-circuit current, I_{SC} experience a jump-like increase from the dark levels to ca. 310 mV and 12 µA, respectively.

As the photocurrent vs. bias dependence remains functionally similar, the increase in the amount of electrical power output of the cell (fourth quadrant of IV-graph) is a result of photovoltaic effects, and not other effects such as photoconduction. It might be tempting to attribute the photo-voltage to the photo-excitation of the defects present within cementitious matrix; however, similarly engineered cells without dye under illumination failed to generate any additional electrical power, which rules out this scenario. Exclusive of the battery effect, the total output power and external device conversion efficiency amount to ~0.35 µW and ~0.001%, respectively. The device fill factor, defined as a ratio of the net maximum power output of the cell to $I_{SC} \times V_{oc}$, is further estimated to be ~0.17 in our case, Figure 4(a).

Discussion

While the obtained results confirm the feasibility of engineering monolithic concrete-DSSC for large-scale solar energy harvesting, it would be beneficial to improve the efficiency and reduce the cost by replacing electrolyte with polymeric thin-films and by further optimizing the cell efficiency. Several factors that are likely contributors to the lower conversion efficiency in our prototypes include a)

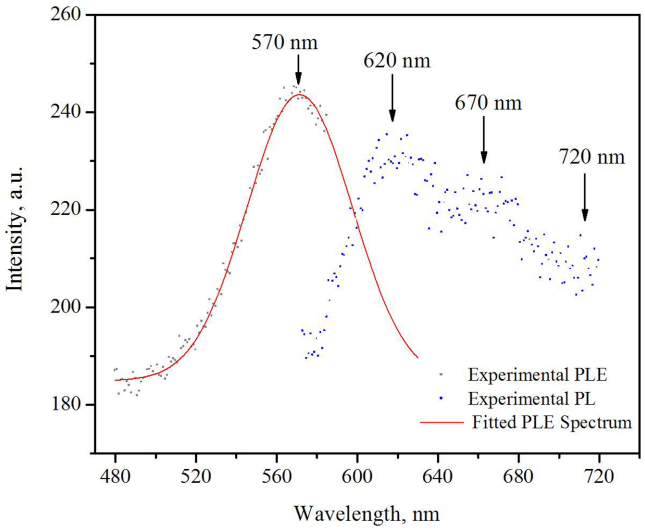

Figure 3 | **The photoluminescence (blue dots) and the photoluminescence excitation (red line) spectra of PGL extract used as light-harvesting component.**

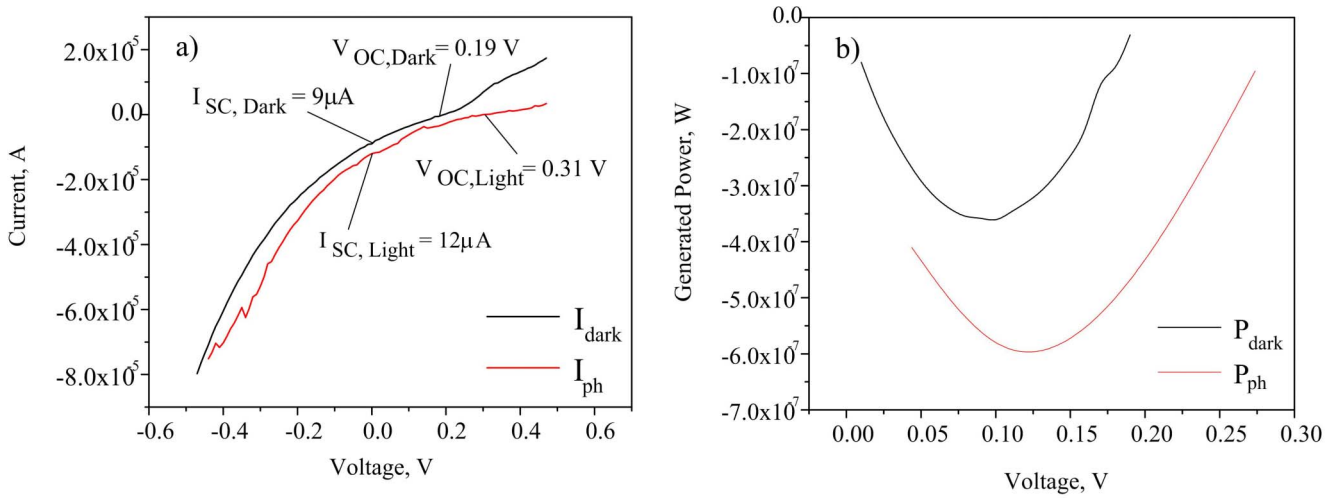

Figure 4 | (a) The I–V characteristic of concrete-dye solar cell in dark (black line), and under illumination (red line). *Punica Granatum* L (PGL) was used as the dye molecule. An increase in the open-circuit voltage and the short-circuit current can be observed upon illumination, resulting in power generation when the cell is exposed to light. (b) Electrical powers vs. voltage obtained under dark and illumination conditions.

un-optimized electrical circuitry of the concrete cell, which accounts for ca. three-fold efficiency drop; b) unoptimized light coupling efficiency; c) luminescence related losses; and d) photo-carrier trap assisted recombination losses. The performance of the cell can be significantly improved by scaling down the TiO_2 layer to lower photo-carrier recombination rates, enhancing the electron transport characteristics of the TiO_2 (via annealing) and concrete matrix, and optimizing light-trapping within the TiO_2 region by proper tailoring the size of TiO_2 particles[15–26]. The concentration of the electron donor (iodide) in the electrolyte is also known to contribute to efficiency and needs to be properly adjusted. The neutralization of oxidized dye-molecules should ideally occur only via the re-dox electrolyte[9,27], yet conduction band electrons can always be recaptured by the oxidized species (tri-iodide) of the electrolyte invoking additional carrier and power losses[22]. Finally, blocking access of the electrolyte to cement matrix is critical to minimize trap-assisted electrolyte recombination current, Figure 1 (right) and to limit the reduction in V_{OC} that occurs internally.

In summary, the concept of a monolithic concrete PV solar cell that can open a door to effective on-site solar-to-electrical energy conversion and power generation by concrete structures was successfully demonstrated. The working cell concept was demonstrated based on prototype comprising a multilayer sandwich featuring an electrically conductive CNT concrete matrix, TiO_2 nanoparticle layer conjugated with dye molecules, iodine electrolyte, and top conductive glass electrode. The current-voltage measurements performed under illumination confirmed successful electrical power generation of a total ~0.64 μW with ~0.35 μW attributed to electrical power directly derived from incident optical power of ~46 mW. The reported work suggests new possibilities in using dye-synthesized titania nanoparticles in combination with concrete technology for future electrical power production within high-density urban environments.

Table 1 | List of the key ingredients and content ratios used to prepare the concrete-based dye solar-cell

Composition	Inner MWCNT Layer	Coating 75NT Layer
WPC %	98.8	25
MWCNT %	1	-
NT %	-	75
PCE %	0.2	-
Water/Powder Ratio	0.5	14

Methods

To engineer a dye-concrete-based solar cell, a homogenous paste of white portland cement (WPC, Type I purchased from Federal) was prepared by mixing with deionized water under ambient conditions. Multi-walled carbon nanotubes (MWCNTs, MW1020 purchased from MKnano) were used at a dosage of ~1% by weight of cement in order to enhance the mechanical strength and conductivity. The MWCNTs had an external diameter of ~10–20 nm and length of ~10–30 μm. Polycarboxylate ether - based superplasticizing admixture (PCE, from Handy Chemicals) was used to improve the workability and dispersion of the MWCNTs within the cement paste. The TiO_2 nanoparticles ($TiO_2 \geq 99.5\%$, NT, Aeroxide P25 from Evonik) with average particle size of ~20 nm and surface area of 50 ± 15 m^2/g were used as a component of the photo-catalytic cement-based coating. According to XRD scans performed on WPC and NT, Figure 2(a), prior to hydration reaction WPC demonstrated a polycrystalline structure that is comprised of crystallites of C_3S, C_2S, and C_3A; at the same time,TiO_2 is shown to include both anatase and rutile phases. A 0.25-mm titanium plate (Ti ≥ 99.7% from Aldrich) was used as a base for the specimens. The surface of the plate was slightly roughened with a 320-grit silicon carbide paper to improve the adhesion of the WPC-MWCNT material, Figure 2 (b-i).

Tablet specimens of ~20 mm in diameter and ~1 mm-thick were cast into a perfusion chamber (PC, supplied by EMS) mounted on the surface of the titanium plate. The WPC-MWCNT tablets were prepared with a water-to-cement ratio of 0.5. MWCNT and PCE were used in the dosage of 1.0 and 0.2% by weight of cement, respectively, as specified in Table 1. Dispersion of the MWCNTs in water was achieved by using PCE as surfactant and by ultrasound (20 kHz) treatment. The PCE was mixed with water at 2000 rpm for 2 min using a high-speed mixer (Silverson L5M-A). The MWCNTs were added and dispersed for 10 minutes using the ultrasound processor (750-W Hielscher UIP1000hd) at 75% of maximum power. Next, containers with the MWCNT dispersion were ultra-sonicated for 10 minutes at 50% power capacity. A water bath filled with ice was used to control the temperature during ultrasonication. WPC was mixed with PCE-MWCNT dispersion for 1 min and a pipette was used to fill the PC molds, Fig. 1(b-ii). Specimens were allowed to harden for 12 hours, after which the PC mold was removed, Fig. 1(b-iii). The specimens were coated with a photo-catalytic WPC-NT layer composed of 75% NT and 25% WPC, Fig. 1(b-iv). A fluid WPC-NT mixture was obtained by intensive stirring at a relatively high water-to-powder ratio of 14. Prior to mixing, the NT powder was added to water and dispersed for 10 minutes using the ultrasound processor at 75% of maximum power (6 W). The WPC-MWCNT tablet specimens were coated with WPC-NT and dried on a hot plate at 50°C.

1. Sobolev, K. & Ferrada, M. How Nanotechnology Can Change the Concrete World, Part 2. *American Ceramic Society Bulletin* **84**, 11, 16–19 (2005).
2. Sanchez, F. & Sobolev, K. Nanotechnology in Concrete - A Review. *Construction and Building Materials* **24**, 11, 2060–2071 (2010).
3. Neville, A. M. Properties of Concrete. Prentice-Hall, Harlow, U.K., 844 (2000).
4. Mehta, P. K. & Monteiro, P. J. M. Concrete: Structure, Properties, and Materials. Prentice Hall, 548 (1993).
5. Bilgen, E. & Richard, M.-A. Horizontal Concrete Slabs as Passive Solar Collectors. *Solar Energy* **72**, 5, 405–413 (2002)

6. Kumar, K. S., Bhaskar, P. U. & Padmakumari, K. Estimation of Land Surface Temperature to Study Urban Heat Island Effect Using Landsat ETM + Image. *International Journal of Engineering Science and Technology* **4**, 2, 771–778 (2012).
7. Flores-Vivian, I., Sobolev, K., Torres-Martinez, L. M., Cuellar, E. L., Valdez, P. L. & Zarazua, E. Performance of Cement Systems with Nano-SiO_2 Particles Produced Using Sol-gel Method. *Journal of the Transportation Research Board* **2141**, 1, 10–14 (2010).
8. Qi, L., Sorge, J. D. & Birnie, D. P. Dye-sensitized solar cells based on TiO_2 coatings with dual size-scale porosity. *J. Am. Ceram. Soc* **92**, 9, 1921–1925 (2009).
9. Grätzel, M. Dye-sensitized solar cells. *Journal of Photochemistry and Photobiology C: Photochemistry Reviews* **4**, 145–153 (2003).
10. Joseph, P. & Tretsiakova-McNally, S. Sustainable Non-Metallic Building Materials. *Sustainability* **2**, 400–427 (2010).
11. George1, R. P., Vishwakarma, V., Samal, S. S. & Mudali, U. K. Current understanding and Future Approaches for Controlling Microbially Influenced Concrete Corrosion: A Review. *Concrete Research Letter* **3**, 3, 491–506 (2012).
12. Nazeeruddin, M. K. *et al. J. Am. Chem. Soc.* **115**, 6382–6390 (1993).
13. Horiuchi, T., Miura, H., Sumioka, K. & Uchida, S. *J. Am. Chem. Soc.* **126**, 12218–12219 (2004).
14. Brouwers, H. & Eijk, R. *Cement and Concrete Research* **33**, 191–196 (2003).
15. Hore, S., Vetter, C., Kern, R., Smit, H. & Hinsch, A. Influence of scattering layers on efficiency of dyesensitized solar cell. *Sol. Energy Mater. Sol. Cells* **9**, 90, 1176–1188 (2006).
16. Barbé, C. J. *et al*. Nanocrystalline titanium oxide electrodes for photovoltaic applications. *J. Am. Ceram. Soc.* **80**, 12, 3157–3171 (1997).
17. Ito, S. *et al*. High-efficiency organic-dye-sensitized solar cells controlled by nanocrystalline-TiO_2 electrode thickness. *Adv. Mater.* **18**, 9, 1202–1205 (2006).
18. Yoon, J. H., Jang, S. R., Vittal, R., Lee, J. & Kim, K. J. TiO_2 nanorods as additive to TiO_2 film for improvement in the performance of dye-sensitized solar cells. *J. Photochem. Photobiol. A.* **180**, 1–2, 184–188 (2006).
19. Wu, B. & Tan, Y. Y. Dye-sensitized solar cells based on anatase TiO_2 nanoparticle/nanowire composites. *J. Phys. Chem. B* **11032**, 15932–15938 (2006).
20. Hu, L. H. *et al*. Microstructure design of nanoporous TiO_2 photoelectrodes for dye-sensitized solar cell modules. *J. Phys. Chem. B* **111**, 2, 358–362 (2007).
21. Hore, S., Nitz, P., Vetter, C., Prahl, C., Niggemann, M. & Kern, R. Scattering spherical voids in nanocrystalline TiO_2 – enhancement of efficieny in dye-sensitized solar cell. *Chem. Commun. (Camb.)* **41**, 15, 2011–2013 (2005).
22. Ferbera, J., Stanglb, R. & Luthera, J. An electrical model of the dye-sensitized solar cell. *Solar Energy Materials and Solar Cells* **53**, 1–2, 29–54 (1998).
23. Luque, A. & Hegedus, S., [ed.]. Handbook of Photovoltaic Science and Engineering. John Wiley & Sons, Ltd (2003).
24. O'Regan, B. & Gratzel, M. A low-cost, high-efficiency solar cell based on dye-sensitized colloidal TiO_2 films. *Nature* **353**, 24 (1991).
25. Sari, K. Sunardi, Characterization of optical properties ofthesansevieria trifasciataextract as dye sensitized solar cells (DSSC). *International Journal of Basic & Applied Sciences IJBAS-IJENS* **11**, 4 (2011).
26. Zhou, H., Wu, L., Gao, Y. & Ma, T. Dye-sensitized solar cells using 20 natural dyes as sensitizers. *Journal of Photochemistry and Photobiology A: Chemistry* **219**, 188–194 (2011).
27. Dai, Q. & Rabani, J. Photosensitization of nanocrystalline TiO_2 films by pomegranate pigments with unusually high efficiency in aqueous medium. *Chem. Commun.* 2142–2143 (2001).

Author contributions

N.K. and K.S. proposed the idea and supervised the research. I.F.V. characterized the materials, produced the specimens and reported on the experimental methods. T.H. carried out the I–V testing and prepared the most of the manuscript text. All authors reviewed the manuscript.

Additional information

Competing financial interests: The authors declare no competing financial interests.

How to cite this article: Hosseini, T., Flores-Vivian, I., Sobolev, K. & Kouklin, N. Concrete Embedded Dye-Synthesized Photovoltaic Solar Cell. *Sci. Rep.* **3**, 2727; DOI:10.1038/srep02727 (2013).

This work is licensed under a Creative Commons Attribution-NonCommercial-NoDerivs 3.0 Unported license. To view a copy of this license, visit http://creativecommons.org/licenses/by-nc-nd/3.0